Carbohydrate Polymers 106 (2014) 49–59

Contents lists available at ScienceDirect

Carbohydrate Polymers

journal homepage: www.elsevier.com/locate/carbpol

Synthesis and characterization of selective thiourea modified Hg(II) ion-imprinted cellulosic cotton fibers

M. Monier*, I.M. Kenawy, M.A. Hashem

Chemistry Department, Faculty of Science, Mansoura University, Mansoura, Egypt

ARTICLE INFO

Article history:
Received 16 December 2013
Received in revised form 17 January 2014
Accepted 21 January 2014
Available online 31 January 2014

Keywords:
Cotton fibers
Cellulose
Thiourea
Ion-imprinting

ABSTRACT

In the present study, Hg^{2+} ion-imprinted chelating fibers based on thiourea modified natural cellulosic cotton fibers (Hg-C-TU) were synthesized and characterized using some instrumental techniques such as elemental analysis, scanning electron microscopy (SEM), FTIR, wide angle X-ray and XPS spectroscopy. The modified Hg-C-TU fibers were employed for selective removal of Hg^{2+} from aqueous solution. Effect of some essential parameters such as pH, temperature, adsorption times and adsorbate concentration were examined to evaluate the optimum adsorption condition. The adsorption kinetics followed the second-order kinetic model indicating that the chemical adsorption is the rate limiting step. Also, the adsorption isotherm experiments showed the best fit with Langmuir model with maximum adsorption capacities 110.3 and 61.8 mg/g for both Hg-C-TU and NI-C-TU, respectively.

1. Introduction

Due to the continuous industrial development, many studies were recently focused on the treatments of the industrial wastes. One of the most important industrial wastes, which mainly cause water pollution, is the heavy metal ions such as mercury, copper, cadmium and palladium. These heavy metals are able to cause serious problems to human, animal and plant life when released into the environment (Hoai, Yoo, & Kim, 2010).

Many common techniques were utilized to get rid of heavy metals from industrial waste water such as chemical precipitation (Espana et al., 2006), ion exchange resins (Fonseca et al., 2005), chitosan derivatives (Monier & Abdel-Latif, 2012), inorganic materials (Dogan et al., 2009; Yavus et al., 2008), and functionalized polymers (Monier & Abdel-Latif, 2013a; Zhou et al., 2009).

Despite the good results obtained by the aforementioned techniques, they are all applied for non-selective heavy metal ion removal. Specific heavy metal ion uptakes provide better environmental protection and also, facilitate the recovery of the removed metal ions, which add an economic value particularly in case of precious metal ions (Hoai et al., 2010).

One of the relatively recent techniques which were employed for enhancing the adsorbent selectivity is the molecular imprinting technique. In this technique, specific recognition sites were created and distributed on the adsorbent matrix, which are able to bind with specific target template molecules/ions on the bases of complex geometry or stereo-chemical configuration (Kara et al., 2004; Krishna et al., 2005; Dakova, Karadjova, Ivanov, Georgieva, Etimova, & Georgiev, 2007; Preetha et al., 2006; Greene, & Shimizu, 2005; Trojanowicz, & Marzena, 2005; Shamsipur, Fasihi, Khanchi, Hassani, Alizadeh, & Shamsipur, 2007).

In the past few years, research interests concern the surface imprinting technique, which provides many advantages such as, better accessibility to the template molecules/ions, simple preparation and higher adsorption capacity. Many studies had been performed for synthesis and preparation of various surfaces ion-imprinted materials for successful and efficient removal of some heavy metal ions such as cadmium and copper (Buhani et al., 2010; Gao et al., 2007), lead (Wang et al., 2009), mercury (Monier & Abdel-Latif, 2013b) and uranyl (Monier & Abdel-Latif, 2013c).

Cellulosic cotton fibers are characterized with various specific advantages such as the high availability, strong mechanical properties, and biodegradability. Due to these characteristic properties, various trials were attempted to improve these original properties and to functionalize cellulose (Nikolic, kostic, praskalo, Pejic, Petronijevic, Skundric, 2010).

Selective periodate oxidation is one of the most common and frequently used techniques for cellulose functionalization (Calvini et al., 2006; Kim et al., 2000; Potthast et al., 2007; Potthast et al., 2009; Varma & Kulkarni, 2002). In this oxidation reaction, the C2—C3 bond of the glucopyranoside ring will be selectively cleaved

* Corresponding author at: Chemistry Department, Faculty of Science, Mansoura University, Mansoura, Egypt, 35516. Tel.: +201003975988.
E-mail address: monierchem@yahoo.com (M. Monier).

0144-8617/$ – see front matter © 2014 Elsevier Ltd. All rights reserved.
http://dx.doi.org/10.1016/j.carbpol.2014.01.074

and converted into two aldehyde groups, which will provide an additional functionality for further cellulose modification with maintaining the mechanical and morphological properties of the fibers (Nikolic et al., 2010).

In this study, thiourea modified Hg^{2+} surface ion-imprinted cotton fibers (C-TU) were prepared and fully characterized using various instrumental techniques. The binding and selectivity studies of the ion-imprinted fibers were performed to optimize the different factors affecting the adsorption behavior such as pH, initial concentration of the Hg^{2+} ions, shaking time, and temperature. The adsorption kinetics and thermodynamic parameters of the uptake process were also calculated.

2. Experimental and methods

2.1. Materials

Cotton fibers were collected from the high agriculture school farm in Mansoura, Egypt and treated by desizing in 1%(v/v) H_2SO_4 and scouring in 1%(w/v) NaOH. The fibers were then washed with distilled water and absolute ethanol and finally the cleaned fibers were dried in an oven at 50 °C till constant weight. Potassium periodate; ethylenediamine; potassium thiocyanate, formaldehyde and $HgCl_2$ were purchased from Sigma–Aldrich. All chemicals were used as received.

2.2. Preparation of the Hg-C-TU ion-imprinted fibers

The ion imprinted Hg-C-TU fibers were synthesized according to the following stepwise procedure.

In the beginning, 0.5 g of the pretreated cotton fibers were soaked in 100 mL 3 g/L aqueous potassium periodate solution and the mixture was gently shaken for 1 h at 50 °C in the dark. Then the oxidized cotton fibers were removed and the remaining periodate oxidant were eliminated by immersing in 100 mL 1% aqueous ethylene glycol solution and stirring the mixture for 30 min. Finally, the fibers were washed with absolute ethanol.

In the next step, the ethanol wet oxidized cotton fibers were then soaked in 100 mL 10% (v/v) alcoholic ethylenediamine solution and the mixture was refluxed at 80 °C for 2 h to produce the ethylenediamine modified cotton (C-EDA). The thiourea (TU) moieties were inserted onto the modified cotton fibers by soaking the previously prepared C-EDA fibers into 100 mL 10% (w/v) potassium thiocyanate aqueous solution, 2 mL 0.5 M HCl solution were added and the mixture was refluxed for 2 h at 80 °C.

The synthetic steps of the cotton modification were schematically presented in Scheme 1.

The obtained C-TU chelating fibers were then loaded with Hg^{2+} by soaking the fibers in 200 mL stopper bottle containing 100 mL 100 mg/L Hg^{2+} solution at pH 5 and 30 °C. The bottle was then shaken for 3 h at 150 rpm.

The ion-imprinting process were then performed by immersing the Hg-C-TU fibers in 100 mL 30% formaldehyde solution and refluxing the mixture for 2 h at 80 °C after adjusting the pH to 5 by adding diluted HCl solution. Finally, the fibers were eliminated from the reaction mixture, washed with distilled water and placed in a conical flask containing 100 mL 0.1 M NHO_3 solution to remove the template Hg^{2+} ions from the cross-linked network of the polymeric matrix. The fibers were then removed, washed with distilled water and dried at 40 °C. For comparison, non-imprinted C-TU fibers (NI-C-TU) were also prepared as a control by the same procedure in absence of the Hg^{2+} ions. The Hg ion imprinting process was schematically presented in Scheme 2.

2.3. Characterization of samples

PerkinElmer 240C Elemental Analytical Instrument (USA) was utilized in performance of the elemental analysis (EA) of the native and modified cotton samples.

Fourier transform infrared (FT-IR) spectrometer (PerkinElmer spectrum) was employed to investigate the infrared spectra of the native and modified cotton fibers using pressed KBr discs.

Scanning electron microscope (FEI Quanta-200 FEI Company, The Netherlands) was utilized for surface morphological evaluation. All the samples were sputter-coated with gold before SEM analysis.

N_2 adsorption isotherm was applied to measure the specific surface area of the samples using an ASAP 2010 Micromeritics instrument and by Brunauer–Emmett–Teller (BET) method.

X-ray powder diffractometer (Japanese Dmax-rA, wavelength = 1.54 Å, CuKα radiation) was performed to determine the crystallinity of native and modified cotton samples. A continuous scan mode was applied to collect $2\theta = 5–60°$.

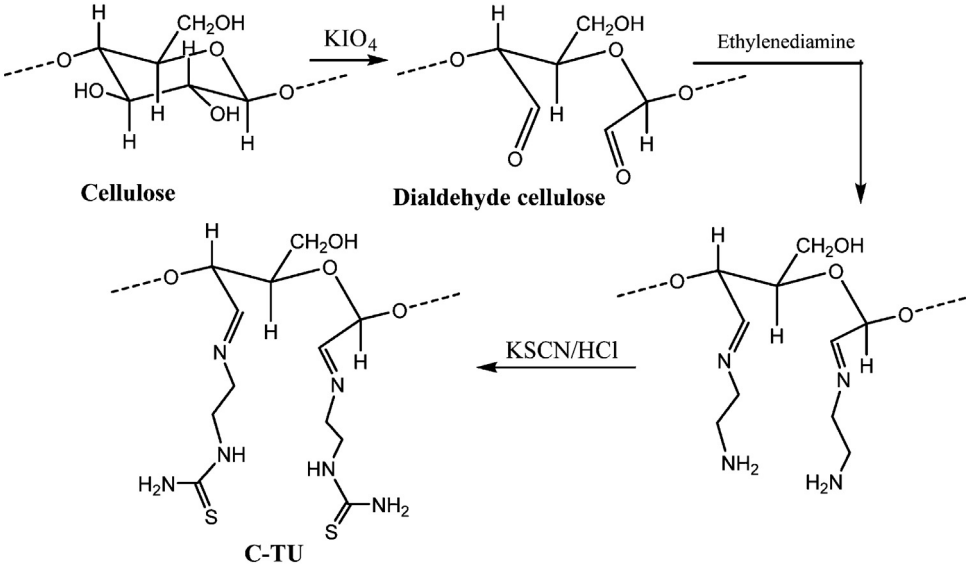

Scheme 1. Synthesis of C-TU chelating fibers.

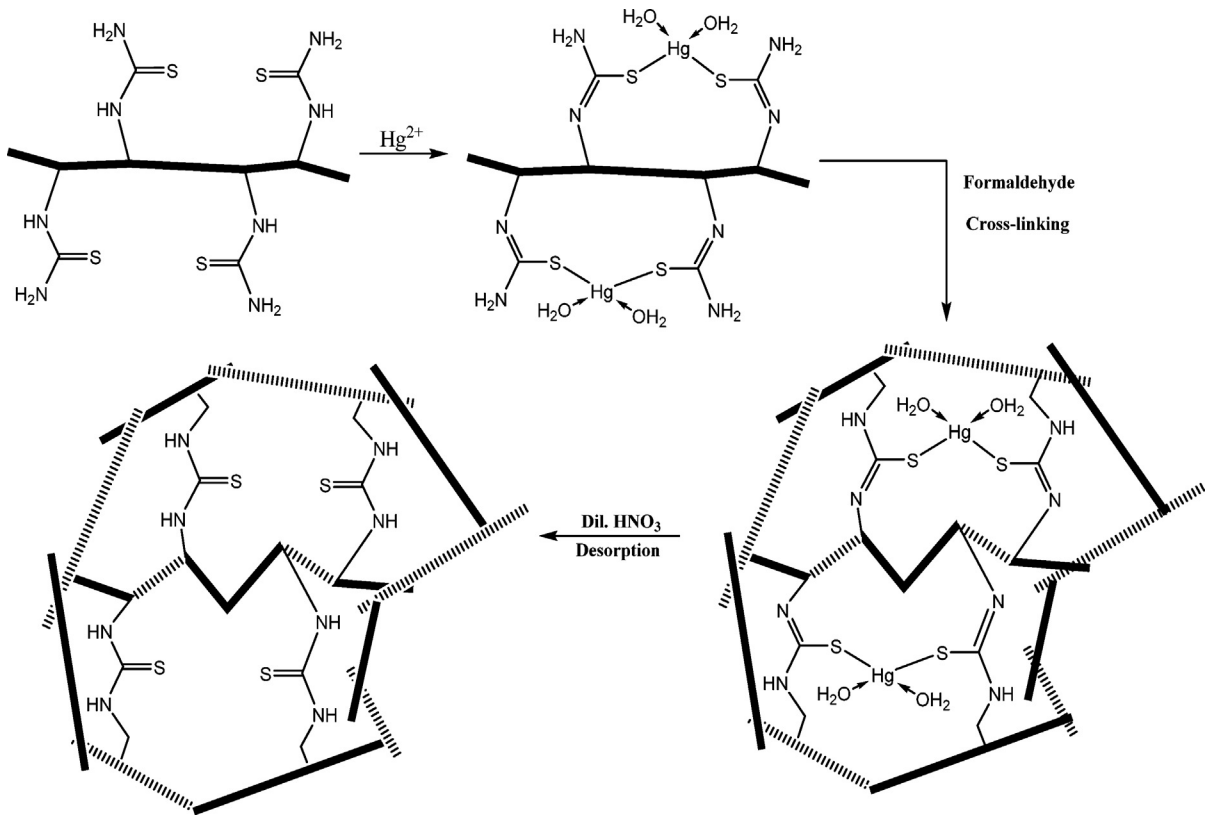

Scheme 2. Ion-imprinting of HG^{2+} ions onto C-TU fibers.

X-ray photoelectron spectrometry (XPS) of the modified and non-modified fibers were performed in FAT mode with the X-ray gun of Mg target (1486.6 eV) at the power of 12 kV × 15 mA, and the analytical background vacuum of 2×10^{-7} Pa, the channel energy of 100 eV and the step length of 0.1 eV/s, using a Kratos XSAM-800 multifunctional spectrometric apparatus (VG Science Instrument Co. Ltd., Britain). The surface of samples were sputtered with the Ar^+ ion to eliminate interference from contaminated substances and subsequently preserved in high vacuum.

2.4. Metal ion uptake experiments using batch method

2.4.1. Instrumentation

A PerkinElmer Model 4100ZL atomic absorption spectrometer was used equipped with a Perkin-Elmer FIAS-400 flow injection system and an AS-90 autosampler. A Perkin-Elmer mercury electrodeless discharge lamp was operated at 180 mA. The mercury absorbance was measured at 253.6 nm with a 0.7 nm spectral bandpass.

2.4.2. Adsorption and desorption experiments

Batch experiments were performed to evaluate the removal of Hg^{2+} ions using both Hg-C-TU ion-imprinted and NI-C-TU non-imprinted fibers. In most of the experiments, 0.03 g of the studied fibers were placed in 100 mL stoppered bottles containing 30 mL Hg^{2+} aqueous solution with main concentration 100 mg/L (except in case of adsorption isotherm studies where the initial Hg^{2+} concentration ranged between 10 and 400 mg/L and thermodynamic studies where the concentration was 30 mg/L), at pH 5 (except for effect of pH studies in which the pH ranged between 1 and 5 using KCl/HCl for pH 1, 2, and 3; CH_3COOH/CH_3COONa for pH 4 and 5), at 30 °C (except for the temperature effect where the temperature ranged between 20 and 40 °C) and for 3 h (except for the kinetic studies where the contact time changed from 10 to 120 min). All the bottles were agitated using orbital shaker at constant rate of 150 rpm. Then, the fibers were eliminated and the residual metal ion content was estimated using atomic absorption.

Both Eq. (1) and Eq. (2) were employed to evaluate the amount of Hg^{2+} adsorbed per one gram of the adsorbent and the percent removal of Hg^{2+}, respectively.

$$q_e = (C_i - C_e)\frac{V}{W} \quad (1)$$

where q_e (mg/g) adsorption capacity; C_i (mg/L) and C_e (mg/L) initial and equilibrated metal ion concentrations, respectively, V (L) volume of added solution and W(g) the mass of the adsorbent (dry).

$$\text{Percentremoval}(\%) = (C_i - C_e) \times \frac{100}{C_i} \quad (2)$$

The desorption experiments of the Hg-C-TU ion imprinted chelating fibers were accomplished using 0.1 M HNO_3 solution as a desorption medium. The desorbed Hg^{2+} amount was measured in desorption medium using atomic absorption.

2.4.3. Selectivity experiments

The competitive removal studies were performed by using a multicomponent mixture containing Cd^{2+}, Pb^{2+}, Cu^{2+}, Co^{2+} in addition to Hg^{2+} each metal ion with initial concentration 20 mg/L. Distribution coefficient (D) calculated using Eq. (3) were utilized for the selectivity evaluation (Birlik et al., 2007).

$$D = [(C_i - C_e)/C_e]\frac{V}{W} \quad (3)$$

The selectivity coefficient is defined as presented in Eq. (4) (Singh & Mishra, 2009).

$$\beta_{Hg^{2+}/M^{n+}} = {D_{Hg}}^{2+}/{D_M}^{n+} \quad (4)$$

Table 1
Elemental analysis of cotton, C-EDA, and C-TU.

Fibers	C(%)	H(%)	O(%)	N(%)	S(%)
Cotton	43.2	6.01	50.69	0	0
C-EDA	50.1	9.5	20.5	19.5	0
C-TU	40.5	7.2	14.1	22.2	15.6

The imprinting effect on the selectivity of the prepared C-TU chelating fibers was evaluated using selectivity coefficient β_r which can be expressed according to Eq. (5) (Liu et al., 2011).

$$\beta_r = \beta_{imprint}/\beta_{non-imprint} \quad (5)$$

where $\beta_{imprint}$ and $\beta_{non\text{-}imprint}$ are the selectivity coefficients of Hg-C-TU and NI-C-TU fibers, respectively.

3. Results and discussion

3.1. Characterization of the polymeric fiber samples

The results obtained from the elemental analysis of native cotton fibers, C-EDA and C-TU are presented in Table 1. As can be seen, upon oxidation and modification of the cotton fibers, the nitrogen and sulfur content exhibited an obvious increase, this finding confirms the insertion of the thiourea moieties onto the oxidized modified cotton fibers. The inserted thiourea units were estimated to be approximately 4.88 mmol g^{-1}.

The morphological structure of the native and modified cotton fibers were visualized by SEM (Fig. 1). As can be observed, the long and narrow streps observed on the oxidized cotton surface (Fig. 1b) could be attributed to the partial corrosion of the fibers upon periodate treatment (Xu et al., 2013). Moreover, the relatively rough and porous surface displayed by the ion-imprinted Hg-C-TU (Fig. 1d) compared to the non-imprinted NI-C-TU fibers (Fig.1c), can be explained as a result of the template Hg^{2+} metal ions removal from the cross-linked network created on the fiber surface. According to the BET surface area measurements, native cotton, Hg-C-TU and NI-C-TU fibers exhibited a surface area 2.432, 7.657 and 3.872 m^2/g, respectively. This relatively low surface area gives an indication that the heavy metal ion adsorption is mainly due to the coordination with the active functional groups inserted onto the fibers.

The consecutive synthetic steps of the C-TU chelating fibers were detected utilizing FTIR spectra, and the results were exhibited in Fig. 2. The spectra of the unmodified cotton fibers (Fig. 2a) exhibited the diagnostic special peaks of the cellulose at approximately 1070–1150 cm^{-1} corresponding to C—O stretching, 1260–1410 cm^{-1} due to O—H bending, and 3600–3100 cm^{-1} due to O—H stretching (Monier & El-Sokkary, 2012). Upon periodate oxidation, the spectrum of the oxidized cotton showed an obvious peak at about 1730 cm^{-1}, which is related to the C═O stretching vibration of the newly formed aldehyde group. After ethylenediamine treatment, the spectrum of C-EDA (Fig. 2c) presents a new peak at approximately 1710 cm^{-1}, which could

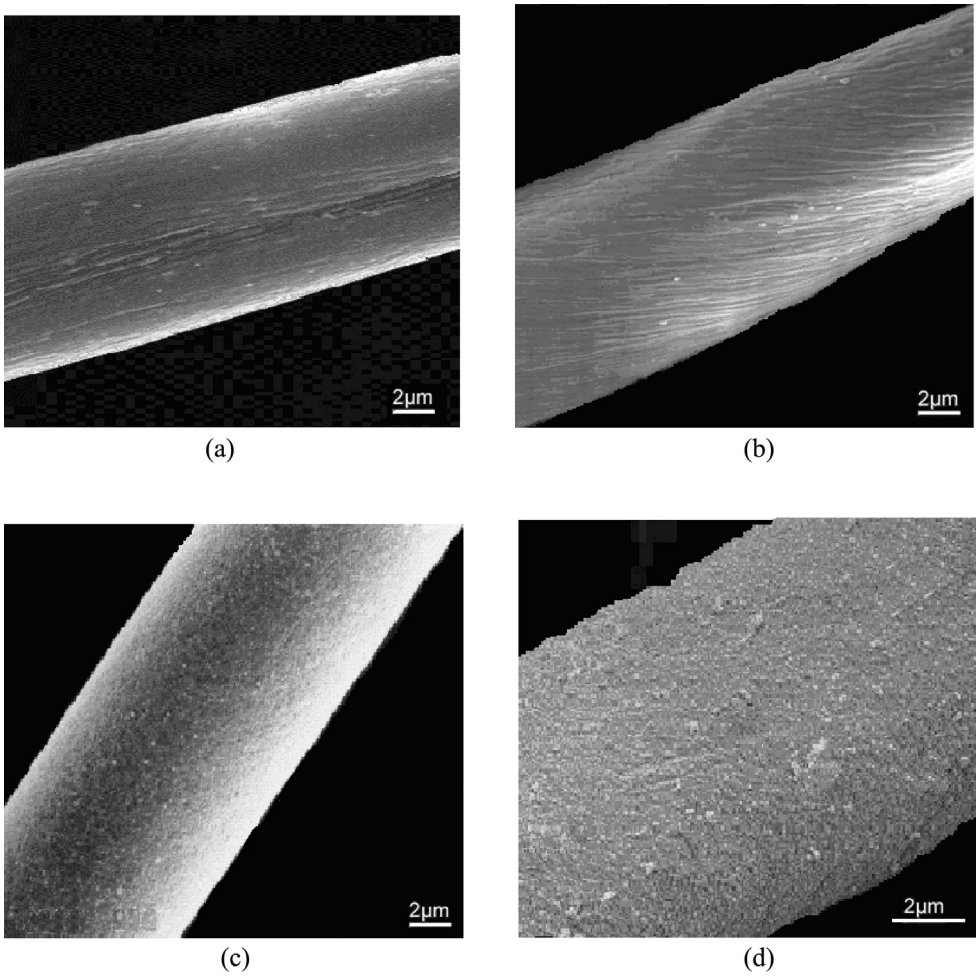

Fig. 1. SEM photos of modified and unmodified cotton fibers. (a) Native unmodified cotton fibers, (b) oxidized cotton fibers, (c) NI-C-TU, and (d) Hg-C-TU.

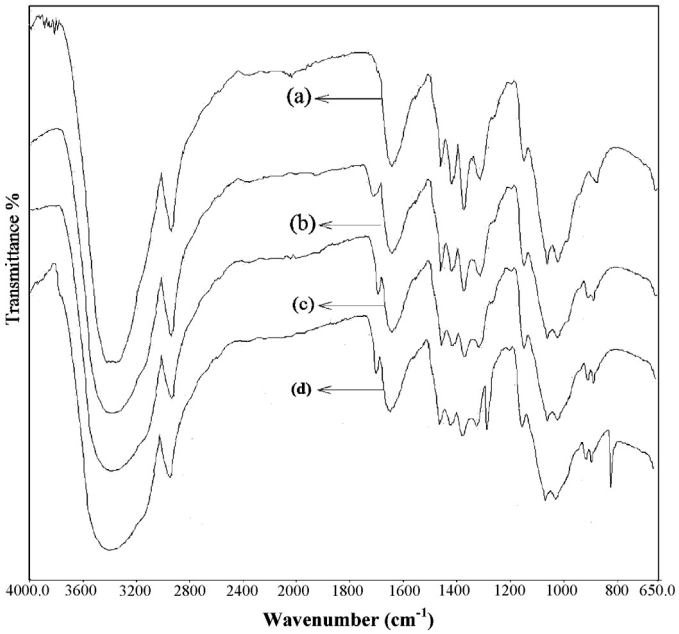

Fig. 2. FTIR spectra of (a) native cotton, (b) oxidized cotton fibers, (c) C-EDA and (d) C-TU.

be attributed to the C=N of the Schiff base formed between the aldehyde group of the oxidized cellulose and the amino group of the ethylenediamine. Furthermore, the spectrum of the finally modified C-TU (Fig. 2d) reveals the insertion of the active thiourea units by the presence of the characteristic peaks at 1290 cm^{-1} and 860 cm^{-1}, which are related to the C=S bond.

As a result of the thioamide group (NH-C=S), thiourea derivatives may undergo thion-thiol tautomerism in solution (Yousef et al., 2013). The absence of the thiol (S—H) and C—S characteristic peaks at approximately 2300 cm^{-1} and 1200 cm^{-1}, respectively in addition to the presence of the sharp C=S peaks at 1290 cm^{-1} and 860 cm^{-1} suggests that the active thiourea units exist mainly in the thion form.

Geometry optimization of the TU derivative moieties inserted onto the modified cotton fibers was performed using MM+ forcefield in HyperChem software version 8.03 implemented on a Dell core i5 personal computer and the molecularly modeled structure was presented in Scheme 3.

The crystalline structure of the modified and native cotton fibers were also investigated utilizing XRD. As presented in Fig. 3, the native cotton fibers exhibited the characteristic crystalline peaks at about 15°, 16° in addition to a sharp intense peak at 23° related to the crystalline phase of cellulose (Xu et al., 2013). On the other hand, the XRD pattern of the modified C-TU chelating fibers (Fig. 3b) didn't show significant changes in the crystalline peaks, which indicates that the aggregating crystalline phase inside the fibers didn't greatly changed after oxidation and modification. However, upon formaldehyde cross-linking (Fig. 3c) the crystalline pattern of the fibers exhibited an obvious decrease, which could be explained as a result of hydrogen bond breaking between the cellulose hydroxyl groups and subsequent creation of more amorphous region.

The native and modified cotton fibers were also examined using X-ray photoelectron spectrometry (XPS). Although the XPS

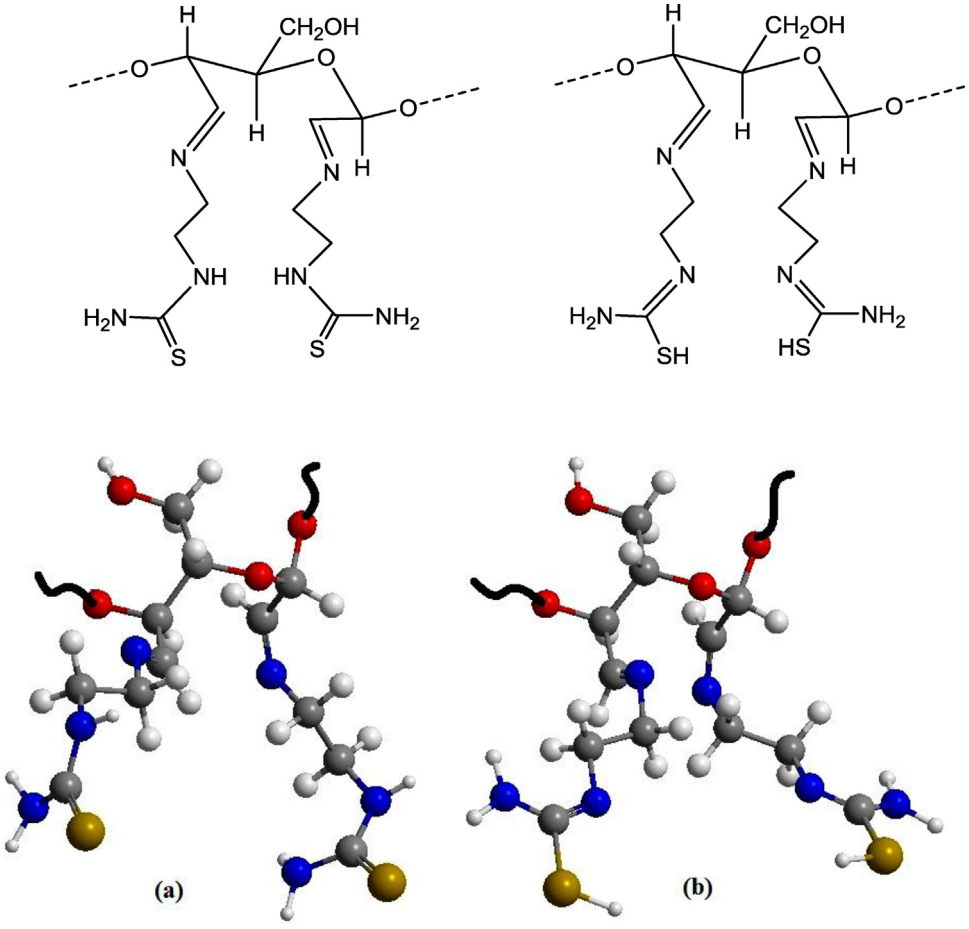

Scheme 3. Molecular modeling of the chelating fibers active center (a) thione form (b) thiol form.

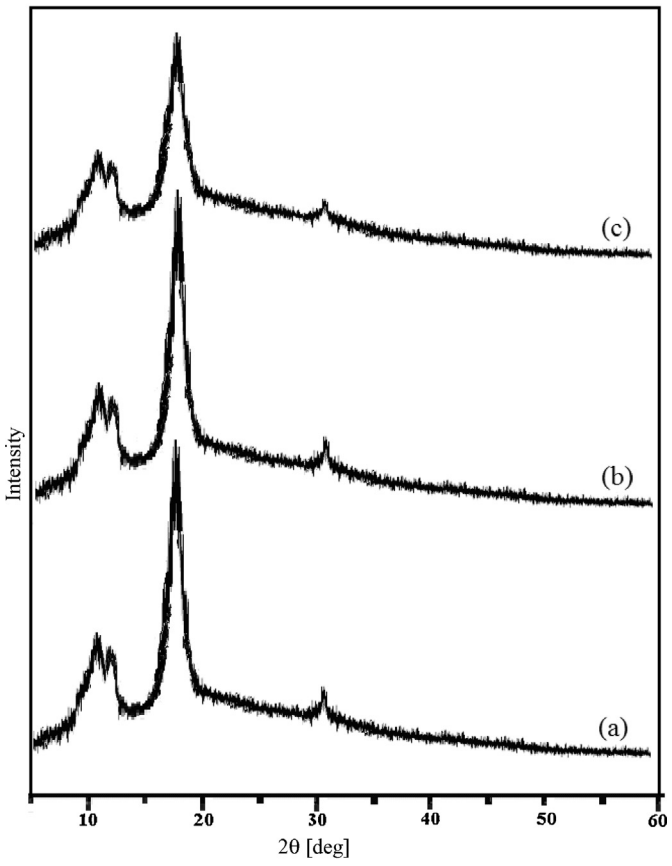

Fig. 3. X-ray diffraction pattern of of (a) native cotton fibers, (b) C-TU, (c) formaldehyde cross-linked C-TU.

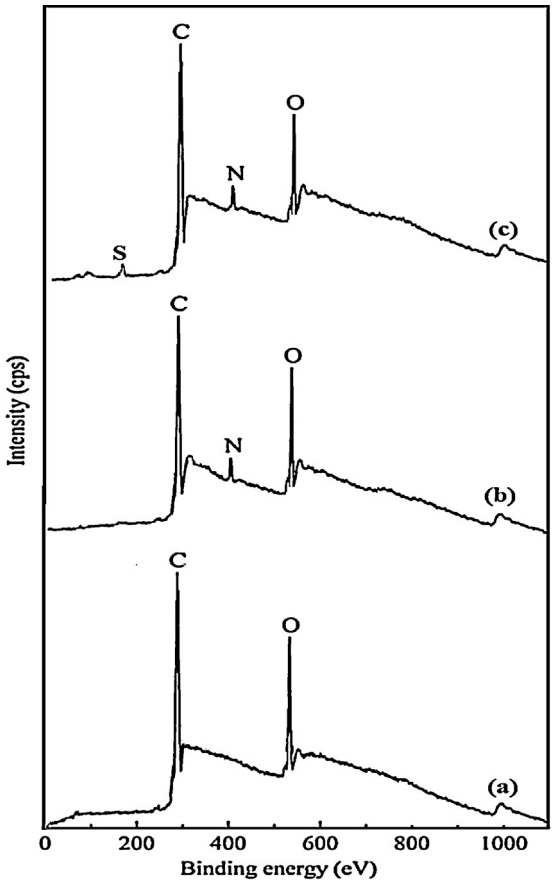

Fig. 4. XPS spectra of: (a) native cotton fibers; (b) C-EDA and (c) C-TU.

spectrum just provides the elemental analysis of the studied fiber surface, it gives a valuable indication about the chemical changes happened during the modifications. The XPS spectrum of native cotton, C-EDA and C-TU are presented in Fig. 4. For the native cotton fibers, only two peaks were observed at 286.5 eV and 531.6 eV corresponding to C and O, respectively (Fig. 4a). After periodate oxidation and subsequent ethylenediamine modification, the XPS spectrum of C-EDA obviously presents a nitrogen specific absorption peak around 402.3 eV as shown in Fig. 4b. Furthermore, the appearance of the S2p peak at 168.8 eV in the spectrum of the modified C-TU chelating fibers presented in Fig. 4c, may also gives an evidence for the insertion of the thiourea moieties onto the modified C-EDA.

3.2. Metal ions uptake studies

3.2.1. Influence of pH

It's previously reported that the initial pH of the aqueous solution plays an essential role in the chemical adsorption of the heavy metal ions (Monier & Abdel-Latif, 2013a). The effect of the initial pH value on the removal of Hg^{2+} using both ion-imprinted Hg-C-TU and non-imprinted NI-C-TU was examined in pH range 1–5, prior to the precipitation limits, and the results were exhibited in Fig. 5. As can be observed, in both cases, the percent removal of Hg^{2+} showed an obvious increase by raising the pH value. Since the Hg^{2+} adsorption is takes place via coordination between the active sites inserted onto the modified cellulosic fibers and the heavy metal cation, at low pH values the majority of the active sites will be protonated, which will subsequently lower the ability of these site to coordinate with Hg^{2+}. In addition, the higher percent removal exhibited by the ion-imprinted Hg-C-TU compared to the non-imprinted NI-C-TU fibers, revealed the selectivity improvement of the ion-imprinting process toward the template target Hg^{2+} ions.

For better evaluation of the mechanism by which the Hg^{2+} can coordinate with the active thiourea units inserted onto the

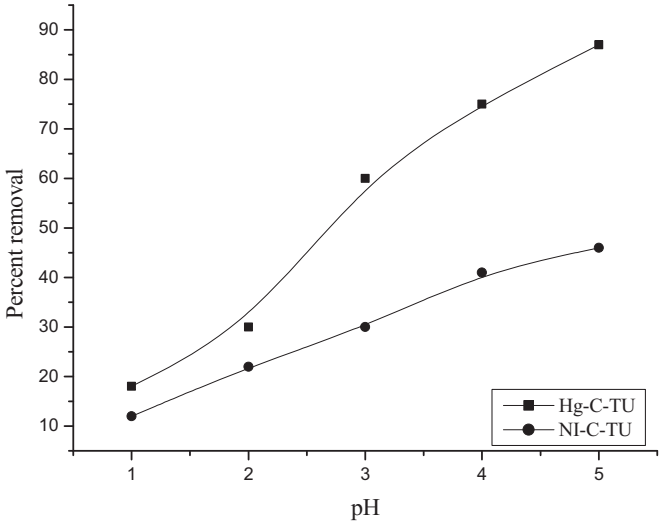

Fig. 5. Effect of pH on the uptake of Hg^{2+} ions by Hg-C-TU and NI-C-TU (initial concentration 100 mg/L; adsorbent. 1 g/L; contact time 3 h; shaking rate 150 rpm, 30 °C).

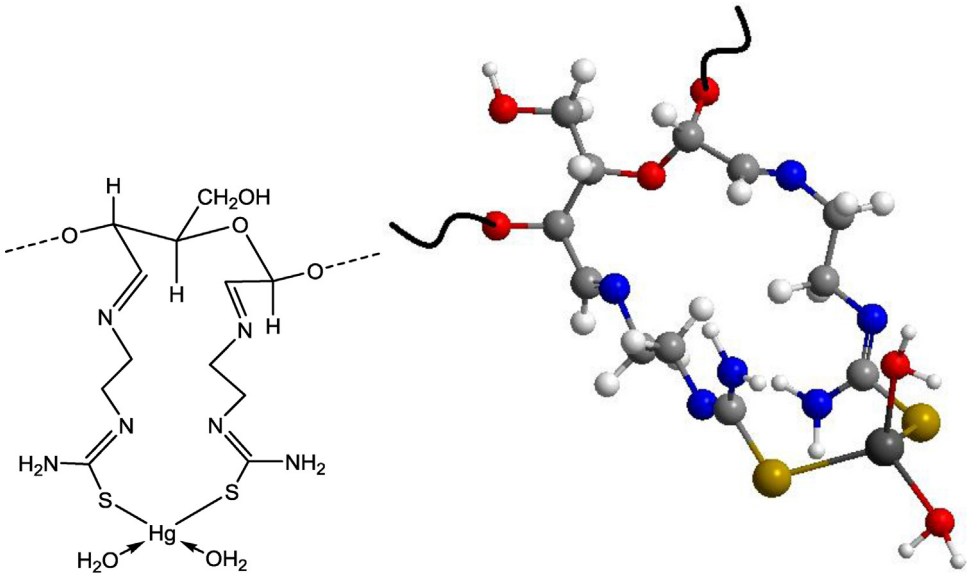

Scheme 4. Molecular modeling of Hg-C-TU.

chelating fibers, the FTIR spectra of the Hg^{2+} loaded C-TU chelating fibers was carried out and compared to the Hg^{2+} free fibers. As expected the main diagnostic thiourea peaks showed obvious changes upon complexation with the Hg^{2+} ions and these changes are presented in Table 2. As can be seen, the absence of v(S—H), v(C=S), appearance of v(C—S) and v(C=N)[b], suggested the coordination via deprotonated thiol groups as shown in the molecularly modeled Scheme 4. This assumption is supported by the obvious lowering of the pH from 5 to about 3 upon Hg^{2+} adsorption.

3.2.2. Thermodynamic studies

The thermodynamic parameters such as free energy ($\Delta G\circ$), enthalpy ($\Delta H\circ$) and entropy ($\Delta S\circ$) of the adsorption process of Hg^{2+} ions using both Hg-C-TU ion-imprinted and NI-C-TU non-imprinted chelating fibers were anticipated by examining the Hg^{2+} removal in a temperature range between 20 and 40 °C. The thermodynamic equilibrium constant (K_C) in addition to the rest of the thermodynamic parameters were calculated according to the following series of equations:

$$K_C = \frac{C_{ad}}{C_e} \quad (6)$$

Table 2
Assignments of characteristic IR spectral peaks (cm^{-1}) of C-TU and Hg-C-TU.

Fibers	v(C=N)[a]	v(C=N)[b]	v/δ(C=S)	v/δ(C—S)
C-TU	1710	–	1290, 860	–
Hg-C-TU	1708	1670	–	1148, 660

[a] Azomethine
[b] New

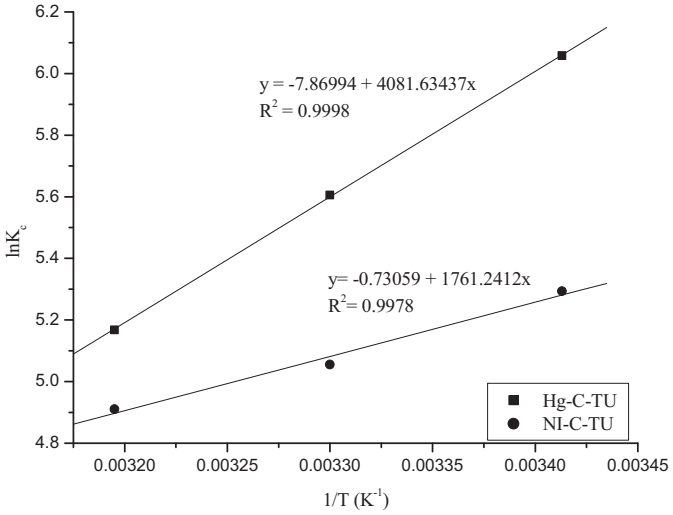

Fig. 6. Plot of lnKC as a function of reciprocal of temperature (1/*T*) for the adsorption of Hg^{2+} by Hg-C-TU and NI-C-TU fibers.

where C_{ad} is the Hg^{2+} concentration adsorbed on the fibers at equilibrium (mg/L) and C_e is the equilibrium concentration (mg/L).

$$\Delta G^\circ_{ads} = -RT\ln K_C \quad (7)$$

$$\ln K_C = \Delta S^\circ_{ads}/R - \Delta H^\circ_{ads}/RT \quad (8)$$

where R (8.314 J/mol K) is the gas constant.

The values of ΔH°_{ads} and ΔS°_{ads} were estimated from the slop ($-\Delta H^\circ_{ads}/R$) and intercept ($\Delta S^\circ_{ads}/R$) of the $\ln K_c$ *vs* $1/T$ plot (Fig. 6).

Table 3
Thermodynamic parameters for the adsorption of Hg^{2+} on Hg-C-TU and NI-C-TU fibers.

System	K_c			$-\Delta G^\circ_{ads}$ (kJ/mol)			ΔH°_{ads}(kJ/mol)	ΔS°_{ads}(J/mol K)
	293 K	303 K	313 K	293 K	303 K	313 K		
Hg-C-TU	427.57	271.73	175.50	14.75	14.12	13.45	−33.93	−65.43
NI-C-TU	199.02	156.89	135.32	12.89	12.77	12.67	−14.64	−6.07

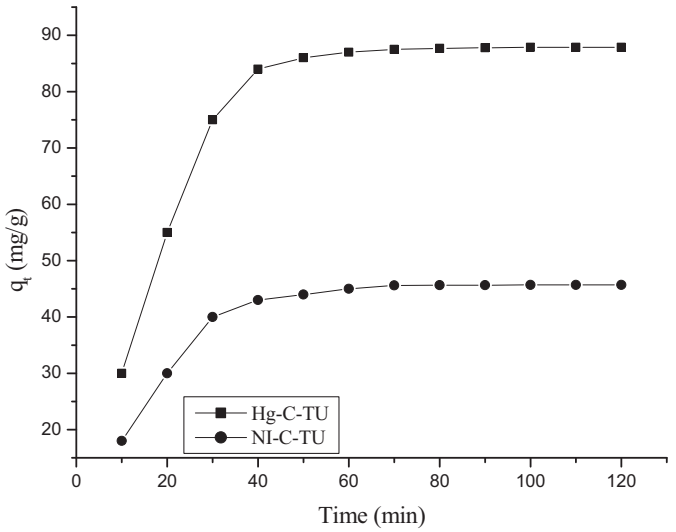

Fig. 7. Effect of contact time on the uptake of Hg^{2+} ions by Hg-C-TU and NI-C-TU fibers (initial concentration 150 mg/L, adsorbent 1 g/L, pH 5.0, shaking rate 150 rpm, 30 °C).

Table 3 lists all the estimated thermodynamic parameters. As can be observed, the exhibited negative ΔG°_{ads} values reveal the thermodynamic feasibility of the adsorption under the studied temperature range. Moreover, the observed ΔG°_{ads} decrease by increasing temperature indicates that the Hg^{2+} removal is favorable at lower temperature.

The adsorption enthalpy is taken as a measurement of the energy barrier that must be crossed by the reacting molecules; the calculated negative ΔH°_{ads} values confirm the exothermic nature of the adsorption process and subsequently, suggest that some amount of heat is lost to the adsorption solution system upon the Hg^{2+} adsorption. In addition, the measured negative ΔS°_{ads} values indicated the lower randomness and higher alignment degree as a result of metal ions adsorption onto the chelating fibers surfaces. Many adsorption systems exhibited a similar behavior (Wang et al., 2012).

3.2.3. Adsorption kinetics

Fig. 7 presents the adsorption kinetics for Hg(II) ions on both Hg-C-TU and NI-C-TU chelating fibers at 30 °C and initial concentration of 100 mg/L from 0 to 120 min. The adsorption rate always slowed down with time elapsed until the adsorption capacity reached a platform after about 30 min adsorption. The equilibrium adsorption capacities of Hg(II) ions onto both Hg-C-TU and NI-C-TU chelating fibers shown in Fig. 7 are 87.5 mg, 45.3 mg per gram of Hg-C-TU and NI-C-TU chelating fibers, respectively, which confirm the selectivity improvement as a result of the imprinting process.

Quantitative kinetics analysis is essential for best designing the adsorption system and well understanding of the adsorption mechanism in addition to identifying the rate limiting step of the adsorption. As a result of various functional groups existence in the modified C-TU chelating fibers such as –NH– and C=S, the chelating fibers may exhibit a various types of interactions. The pseudo-first-order equation (Eq. (9)) and the pseudo-second-order equation (Eq. (10)) are the most frequently used in the kinetic analysis of adsorption.

$$\frac{1}{q_t} = \frac{k_1}{q_e t} + \frac{1}{q_e} \quad (9)$$

$$\frac{t}{q_t} = \frac{1}{k_2 q_e^2} + \left(\frac{1}{q_e}\right) t \quad (10)$$

Table 4
Kinetic parameters for Hg^{2+} adsorption by Hg-C-TU and NI-C-TU fibers.

Fibers	First-order model		
	k_1 (min^{-1})	q_{e1}(mg/g)	R^2
Hg-C-TU	7.786	90 ± 3	0.9134
NI-C-TU	5.678	46 ± 4	0.9265
Fibers	Second-order model		
	k_2 (g/(mg min))	q_{e2}(mg/g)	R^2
Hg-C-TU	4.8 x 10^{-3}	87 ± 1	0.9998
NI-C-TU	3.9 x 10^{-3}	45 ± 1	0.9987

where q_e (mg/g) and q_t (mg/g) are the adsorption capacities at equilibrium and at time t (min), respectively. k_1 is the rate constant of pseudo-first-order adsorption, k_2 the rate constant of pseudo-second-order adsorption.

For both models, k and q_e were usually calibrated together and the closes to the experimental adsorption data in addition to the correlation coefficient were utilized to evaluate the best kinetic model fits with the experimental work. Table 4 lists the kinetic parameters for the studied models and as can be noticed pseudo-second-order equation exhibited the best fit with the experimental data.

Generally, the adsorption and desorption process in solution could be presented as in the following:

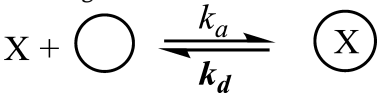

where, X is the adsorbate k_a is the adsorption rate constant, k_d the desorption rate constant, and O represents the active adsorption site. Actually, the adsorption of heavy metal ions onto porous materials takes place via three steps; (i) diffusion of the metal ions from the bulk of solution to the adsorbent surface; (ii) diffusion of the metal ions into the material pores; (iii) chemical adsorption of the metal ions on the active sites of the adsorbent material. The validity of the pseudo-second-order equation may support the surface chemical adsorption as a rate-controlling mechanism. In addition, the initial adsorption rate can be calculated from k_2 and q_e according to the pseudo-second-order model are 2.75 and 1.51 mg/(g min) for Hg-C-TU and NI-C-TU, respectively. Many previous adsorption studies exhibited a fit of the experimental data with the second-order model, for example; removal of Hg(II), Cd(II) and Zn(II) ions using phenylthiourea modified chitosan (Monier & Abdel-Latif, 2012), removal of Cu^{2+} and Cr^{2+} using modified polyacrylonitrile composites (Yavus et al., 2008), adsorption of Cu^{2+} using modified ion-imprinted polymethacrylic microbeads (Dakova et al., 2007) and adsorption of uranyl using ion-imprinted polymeric particle (Preetha et al., 2006).

3.2.4. Adsorption isotherms

The adsorption isotherm studies are very important to explain the interaction between the Hg^{2+} metal ions and both Hg-C-TU ion-imprinted and NI-C-TU non-imprinted chelating fibers and either theoretical or empirical models are utilized for correlation with the equilibrium adsorption data in order to design the adsorption system. Both Freundlich (Eq. (11)) and Langmuir (Eq. (12)) are the most commonly employed isotherm models.

$$\ln q_e = \ln K_F + \frac{1}{n}(\ln C_e) \quad (11)$$

$$\frac{C_e}{q_e} = \left(\frac{1}{K_L q_m}\right) + \left(\frac{C_e}{q_m}\right) \quad (12)$$

Table 5
Parameters for Hg^{2+} ions adsorption by Hg-C-TU and NI-C-TU fibers according to different equilibrium models.

Fibers	Langmuir isotherm constants		
	K_L(L/g)	q_m(mg/g)	R^2
Hg-C-TU	21.5 x 10^{-2}	110.3	0.9989
NI-C-TU	12.3 x 10^{-2}	61.8	0.9999
Fibers	Freundlich isotherm constants		
	K_F	n	R^2
Hg-C-TU	23.111	2.986	0.8788
NI-C-TU	15.213	3.101	0.9087

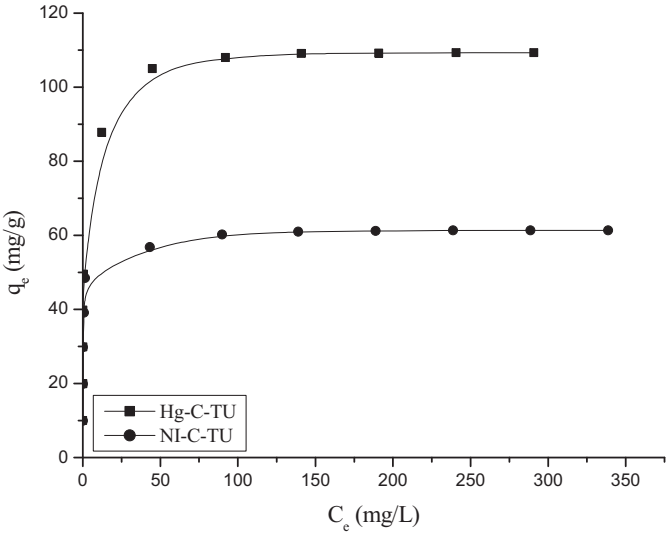

Fig. 8. Adsorption isotherms of Hg^{2+} ions by Hg-C-TU and NI-C-TU fibers (initial concentration 10–400 mg/L, adsorbent 1 g/L, pH 5.0, shaking rate 150 rpm, 30 °C).

where, q_e is the adsorption capacity of metal ions at equilibrium (mg/g), C_e the metal ions concentration in solution (mg/L) at equilibrium, K_F (L/mg) the Freundlich constant, $1/n$ the heterogeneity factor. The K_L (L/mg) and q_m(mg/g) are the Langmuir coefficients, representing the adsorption equilibrium constant and the monolayer capacity, respectively.

According to Langmuir model, the adsorpate will form a monolayer on energetically homogeneous surface and no interaction between the adsorbent. On the other hand, Freundlich model describes the adsorption on heterogeneous surface on which the adsorbed molecules are interactive.

The adsorption isotherm experiments were performed at 30 °C and the equilibrium concentration of the metal ion in solution correlated with the adsorption capacity. As can be seen in Fig. 8, the adsorption capacities for both Hg-C-TU and NI-C-TU exhibited an obvious increase with increasing the metal ion concentration until reaching saturation.

The obtained experimental data were employed with both Langmuir and Freundlich isotherm model and all the parameters were summarized in Table 5. As can be seen, from the correlation coefficient values Langmuir model exhibited the best fit for the adsorption equilibrium experimental data, which very well implies the monolayer adsorption pattern on energetically uniform surface. The maximum adsorption capacities for both Hg-C-TU and NI-C-TU were 110.3 and 61.8 mg/g. The higher capacity for the ion-imprinted compared to the non-imprinted fibers could be explained as a result of both the higher surface area and the imprinting effect.

The suitability of the adsorption process could be evaluated by calculating the separation factor constant (R_L): $R_L > 1.0$, unsuitable; $R_L = 1$, linear; $0 < R_L < 1$, suitable; $R_L = 0$, irreversible (Zhou et al., 2012). The R_L value can be estimated according to the following equation:

$$R_L = \frac{1}{(1 + C_0 K_L)} \quad (13)$$

where K_L is the Langmuir equilibrium constant and C_0 (10–400 mg/L) is the initial concentration of the Hg(II) ions. The values of R_L lie between 0.0116 and 0.317, indicating the suitability of the imprinted fibers as adsorbents for Hg(II) from aqueous solution.

In out previous work (Monier & Abdel-Latif, 2012; Monier & Abdel-Latif 2013a; Monier & Abdel-Latif 2013b), in addition to other studies in literature (Esmaili-Sari, Anbia, Younesi, Amirmahmoodi, & Ghafari-Nazari, 20011; Cui et al., 2013) where Hg^{2+} ions were adsorbed using modified chitosan, chelating fibers based on PET, modified mesoporous carbon and amine-modified attapulgite, the adsorption isotherms followed Langmuir model which is in agreement with the present study.

3.2.5. Selectivity studies

As the selectivity studies are essential in this work, the selectivity of both Hg-C-TU and NI-C-TU were evaluated by the competitive adsorption of Hg^{2+} in a multi-component solution mixture containing Cd^{2+}, Pb^{2+}, Cu^{2+}, Co^{2+} and Hg^{2+}. The distribution ratio and the selectivity coefficients of Hg^{2+} compared to the other metal ions are presented in Table 6. As can be seen, Hg-C-TU presents a distribution coefficient about 35 times greater than that of NI-C-TU. In addition, the ion-imprinted Hg-C-TU exhibited a relative selectivity coefficient greater than 1 for each metal. These results can be explained because of the creation of selective restricted

Table 6
Selective adsorption of Hg(II) from multicomponent mixtures by Hg-C-TU and NI-C-TU (initial concentration 20 mg/L, adsorbent 1 g/L, shaking rate 150 rpm, solution pH 5.0, 30 °C).

Metal	Distribution ratio (L/g)		Selectivity coefficient $\beta_{Hg^{2+}/M^{n+}}$		Relative selectivity coefficient β_r
	Hg-C-TU	NI-C-TU	Hg-C-TU	NI-C-TU	
Hg^{2+}	435.22	12.43	–	–	
Cd^{2+}	6.21	11.65	70.08	1.06	66.11
Pb^{2+}	6.36	14.87	68.43	0.83	82.44
Cu^{2+}	5.68	9.32	76.62	1.33	57.61
Co^{2+}	1.77	2.13	245.88	5.83	42.17

Table 7
Repeated adsorption of Hg^{2+} ions by Hg-C-PTS (initial concentration 100 mg/L, Hg-C-TU 1 g/L, pH 5.0, contact time 3 h, shaking rate 150 rpm, 30 °C)

Cycle number	Adsorption capacity (%)
1	100
2	98
3	95
4	93
5	91

coordination sites based on the geometry of the Hg^{2+} complex, which are relatively able to rebind with Hg^{2+} ions more than any other metal ions.

3.2.6. Reusability of fibers

For examining the chelating fibers reusability, five adsorption-desorption cycles had been performed under optimum conditions as previously described in Section 2.4.2 and the results were presented in Table 7. It's obvious that the adsorption efficiency of the Hg-C-TU ion-imprinted chelating fibers didn't show a significant decrease. After the fifth cycle, the fibers maintain about 91% of its original efficiency. According to these results, it's expected that the prepared fibers would be a promising adsorbent for fast selective removal of Hg^{2+} from water, especially in emergency disposal of heavy metal pollution accidents.

4. Conclusions

In this work, a novel highly selective Hg(II) ion-imprinted thiourea modified cellulosic cotton chelating fibers (Hg-C-TU) were prepared and characterized using various instrumental techniques. The adsorption kinetics of Hg^{2+} onto Hg-C-TU was fast and followed the pseudo-second order model confirming the adsorption through the chemical coordination mechanism. Also, Langmuir isotherm model was well fitted with the experimental data, implying the monolayer adsorption of Hg^{2+} ions. In addition, the thermodynamic studies indicated that the adsorption was exothermic in nature and spontaneous at all studied temperatures. Competitive adsorption studies showed that Hg^{2+} offers the advantages of selectivity toward targeted Hg^{2+} compared with the NI-C-TU even in presence of other metal ions.

References

Birlik, E., Ersoz, A., Acykkalp, E., Denizli, A., & Say, R. (2007). Cr (III)-imprinted polymeric beads: sorption and preconcentration studies. *Journal of Hazardous Materials B*, *140*, 110–116.

Buhani, Narsito, Nuryono, & Kunarti, E. S. (2010). Production of metal ion imprinted polymer from mercapto-silica through sol–gel process as selective adsorbent of cadmium. *Desalination*, *251*, 83–89.

Calvini, P., Conio, G., Princi, E., Vicini, S., & Pedemonte, E. (2006). Viscometric determination of dialdehyde content in periodate oxycellulose Part II. Topochemistry of oxidation. *Cellulose*, *13*, 571–579.

Cui, H., Qian, Y., Li, Q., Wei, Z., & Zhai, J. (2013). Fast removal of Hg(II) ions from aqueous solution by amine-modified attapulgite. *Applied Clay Science*, *72*(2013), 84–90.

Dakova, I., Karadjova, I., Ivanov, I., Georgieva, V., Etimova, B., & Georgiev, G. (2007). Solid phase selective separation and preconcetration of Cu(II) by Cu(II)-imprinted polymethacrylic microbeads. *Analytica Chimica Acta*, *584*, 196–203.

Dogan, M., Turkyilmaz, A., Alkan, M., & Demirbas, O. (2009). Adsorption of copper (II) onto sepiolite and electrokinetic properties. *Desalination*, *238*, 257–270.

Espana, J. S., Pamo, E. L., Pastor, E. S., Andres, J. R., & Rubi, J. A. M. (2006). The removal of dissolved metals by hydroxysulphate precipitates during oxidation and neutralization of acid mine waters. *Aquatic Geochemistry*, *12*, 269–298.

Fonseca, M. G., Oliveora, M. M., Arakaki, L. N. H., Espinola, J. G. P., & Airoldi, C. (2005). Natural vermiculite as an exchanger support for heavy cat in aqueousIn. *Journal of Colloid and Interface Science*, *285*, 50–55.

Gao, B. J., An, F. Q., & Zhu, Y. (2007). Novel surface ionic imprinting materials prepared via couple grafting of polymer and ionic imprinting on surfaces of silica gel particles. *Polymer*, *48*, 2288–2297.

Greene, N. T., & Shimizu, K. D. (2005). Colorimetric molecularly imprinted polymer sensor array using dye displacement. *Journal of the American Chemical Society*, *127*, 5695–5700.

Hoai, N. T., Yoo, D.-K., & Kim, D. (2010). Batch and column separation characteristics of copper-imprinted porous polymer micro-beads synthesized by a direct imprinting method. *Journal of Hazardous Materials*, *173*, 462–467.

Kara, R., Biju, J. V., & Rao, T. P. (2004). Influence of binary/ternary complex of imprint ion on the preconcentration of uranium(IV) using ion imprinted polymer materials. *Analytica Chimica Acta*, *512*, 63–73.

Kim, U.-J., Kuga, S., Wada, M., Okano, T., & Kondo, T. (2000). Periodate oxidation of crystalline cellulose. *Biomacromolecules*, *1*, 488–492.

Krishna, P. G., Gladis, J. M., Rao, T. P., & Naidu, G. R. (2005). Selective recognition of neodymium (III) using ion imprinted polymer particles. *Journal of Molecular Recognition*, *18*, 109–116.

Liu, B., Wang, D., Li, H., Xu, Y., & Zhang, L. (2011). As(III) removal from aqueous solution using α-Fe_2O_3 impregnated chitosan beads with As(III) as imprinted ions. *Desalination*, *272*(2011), 268–292.

Monier, M., & Abdel-Latif, D. A. (2012). Preparation of cross-linked magnetic chitosan-phenylthiourea resin for adsorption of Hg(II), Cd(II) and Zn(II) ions from aqueous solutions. *Journal of Hazardous Materials*, *209-210*, 240–249.

Monier, M., & Abdel-Latif, D. A. (2013a). Modification and characterization of PET fibers for fast removal of Hg(II), Cu(II) and Co(II) metal ions from aqueous solutions. *Journal of Hazardous Materials*, *250/251*, 122–130.

Monier, M., & Abdel-Latif, D. A. (2013b). Synthesis and characterization of ion-imprinted chelating fibers based on PET for selective removal of Hg^{2+}. *Chemical Engineering Journal*, *221*, 452–460.

Monier, M., & Abdel-Latif, D. A. (2013c). Synthesis and characterization of ion-imprinted resin based on carboxymethyl cellulose for selective removal of UO_2^{2+}. *Carbohydrate Polymers*, *97*, 743–752.

Monier, M., & El-Sokkary, A. M. A. (2012). Modification and characterization of cellulosic cotton fibers for efficient immobilization of urease. *International Journal of Biological Macromolecules*, *51*, 18–24.

Nikolic, T., Kostic, M., Praskalo, J., Pejic, B., Petronijevic, Z., & Skundric, P. (2010). Sodium periodate oxidized cotton yarn as carrier for immobilization of trypsin. *Carbohydrate Polymers*, *82*, 976–981.

Potthast, A., Kostic, M., Schiehser, S., Kosma, P., & Rosenau, T. (2007). Studies on oxidative modifications of cellulose in the periodate system: Molecular weight distribution and carbonyl group profiles. *Holzforschung*, *61*, 662–667.

Potthast, A., Schiehser, S., Rosenau, T., & Kostic, M. (2009). Oxidative modifications of cellulose in the periodate system–reduction and beta-elimination reactions. *Holzforschung*, *63*, 12–17.

Preetha, C. R., Gladis, J. M., & Rao, T. P. (2006). Removal of toxic uranium from synthetic nuclear power reactor effluents using uranyl ion imprinted polymer particles. *Environmental Science and Technology*, *40*, 3070–3074.

Shamsipur, M., Fasihi, J., Khanchi, A., Hassani, R., Alizadeh, K., & Shamsipur, H. (2007). A stoichiometric imprinted chelating resin for selective recognition of copper(II) ions aqueous media. *Analytica Chimica Acta*, *599*, 294–301.

Singh, D. K., & Mishra, S. (2009). Synthesis and characterization of UO_2^{2+}-ion imprinted polymer for selective extraction of UO_2^{2+}. *Analytica Chimica Acta*, *644*, 42–47.

Trojanowicz, M., & Marzena, W. (2005). Electrochemical and piezoelectric enantioselective sensors and bioselective sensors. *Analytical Letters.*, *38*, 523–547.

Varma, A. J., & Kulkarni, M. P. (2002). Oxidation of cellulose under controlled conditions. *Polymer Degradation and Stability*, *77*, 25–27.

Wang, J., Xu, L., Cheng, C., Meng, Y., & Li, A. (2012). Preparation of new chelating fiber with waste PET as adsorbent for fast removal of Cu^{2+} and Ni^{2+} from water: Kinetic and equilibrium adsorption studies. *Chemical Engineering Journal*, *193-194*, 31–38.

Wang, L. M., Zhou, M. H., Jing, Z. J., & Zhong, A. (2009). Selective separation of lead from aqueous solution with a novel Pb (II) surface ion-imprinted sol–gel sorbent. *Microchimica Acta*, *165*, 367–372.

Xu, Y., Huang, C., & Wang, X. (2013). Characterization and controlled release aloe extract of collagen protein modified cotton fiber. *Carbohydrate Polymers*, *92*, 982–988.

Yavus, M., Gode, F., Phelivan, E., Ozmert, S., & Sharma, Y. C. (2008). An economic removal of Cu^{2+} and Cr^{2+} on the new adsorbents: pumice and polyacrylonitrile/pumice composite. *Chemical Engineering Journal*, *137*, 453–461.

Yousef, T. A., Abu El-Reash, G. M., El-Gammal, O. A., & Bedier, R. A. (2013). Synthesis, characterization, optical band gap, in vitro antimicrobial activity and DNA cleavage studies of some metal complexes of pyridyl thiosemicarbazone. *Journal of Molecular Structure*, *1035*, 307–317.

Zhou, L., Shang, C., Liu, Z., Huang, G., & Adesina, A. A. (2012). Selective adsorption of uranium(VI) from aqueous solutions using the ion-imprinted magnetic chitosan resins. *Journal of Colloid and Interface Science*, *366*, 165–172.

Zhou, L. C., Li, Y. F., Bai, X., & Zhao, G. H. (2009). Use of microorganisms immobilized on composite polyurethane foam to remove Cu(II) from aqueous solution. *Journal of Hazardous Materials*, *167*, 1106–1113.

Zolfaghari, G., Esmaili-Sari, A., Anbia, M., Younesi, H., Amirmahmoodi, S., & Ghafari-Nazari, A. (2011). Taguchi optimization approach for Pb(II) and Hg(II) removal from aqueous solutions using modified mesoporous carbon. *Journal of Hazardous Materials*, *192*, 1046–1055.